Density of states in the vortex state of type-II superconductors

U. Klein
Institut für Theoretische Physik der Universität Linz, A-4040 Linz-Auhof, Austria
(Received 8 May 1989)

The local, direction resolved density of states in the vortex state of clean type-II superconductors is calculated for arbitrary energies and inductions. It is obtained by solving numerically the quasiclassical equations of superconductivity, using parameters corresponding to Nb or V. The excitation spectrum is discussed for arbitrary inductions and, for the special case of large vortex distance, compared with previous theories. Tunneling states of quasiparticles are calculated explicitly for the first time and a shift of continuum states to energies higher than $\psi_{\rm BCS}$ is found. Some conclusions specific to the important materials Nb and V are drawn. The energy dependence of the local density of states near the vortex axis is found to be in qualitative agreement with recent scanning-tunneling-microscope measurements.

I. INTRODUCTION

Up to now the electronic density of states of a clean type-II superconductor in the mixed state has been calculated only in a few limiting cases. These include the limit of large flux-line distance (isolated flux line) where two different energy ranges have been investigated. First, the range of energies[1-5] much smaller than the Meissner-state order parameter, $E \ll |\psi_{\rm BCS}|$, and, second, the range of the continuum states, $E > |\psi_{\rm BCS}|$. In all these papers[1-7] either independent or nearly independent[5] flux lines have been considered. Interacting flux lines have only been treated[8-10] for applied fields close to the upper critical field H_{c2}. We should also mention that the use of not self-consistently determined "potentials" (order parameter and vector potential is a common feature of all previous theories.

The previously mentioned work led to considerable theoretical insight in several important limiting cases (some comments on the experimental situation will be given at the end of this paper). Nevertheless, a theoretical description of the density of states of the vortex state of clean type-II superconductors for the most part is still missing. In particular, one of the yet unanswered questions is to what extent results of independent flux-line theories may be applied to the low-field region of actually existing clean type-II superconductors like Nb and V. In these low-κ materials, as is well known, the maximal flux-line distance is limited by vortex attraction. The phenomenon of vortex attraction[11] has recently been reconsidered in a number of experimental[12,13] and theoretical papers.[14-16,13]

In the present paper some results of a self-consistent calculation of the density of states for arbitrary energy and flux-line distance are reported. More precisely, we address ourselves to the quantity $N(E,\mathbf{k},\mathbf{r})$ which is the local, direction-dependent tunneling density of states for quasiparticle excitations of energy E and direction $\mathbf{k}$ ($\mathbf{k}$ is a unit vector) at point $\mathbf{r}$. For simplicity, we will frequently refer to this quantity as "density of states" in what follows. From $N(E,\mathbf{k},\mathbf{r})$ one can obtain the local density of states $N(E,\mathbf{r})$ and the total density of states $N(E)$ by averaging with respect to all directions $\mathbf{k}$ and space points $\mathbf{r}$. However, in this work we restrict ourselves almost exclusively to a discussion of the basic quantity $N(E,\mathbf{k},\mathbf{r})$.

A measurable quantity is the direction-dependent tunneling conductance $\sigma(V,\mathbf{k},\mathbf{r})$ which is defined as the convolution of $N(E,\mathbf{k},\mathbf{r})$ and the derivative of the Fermi distribution function. Recently, a weighted average (with respect to $\mathbf{k}$) of $\sigma(V,\mathbf{k},\mathbf{r})$ has been observed in a scanning-tunneling-microscope experiment.[17] Such measurements yield, for the first time, information on the local density of states of a superconductor in the mixed state.

The density of states will be calculated by means of the Green's-function formalism, which is equivalent to the Bogoliubov method in the clean limit. In Sec. II we recall the quasiclassical, or Eilenberger equations[18] and discuss the numerical methods used to obtain a vortex lattice solution of these equations. Readers only interested in results may skip this section except for the parts of it referring to the notation.

Section III contains a discussion of the numerical results. We first consider the case of an isolated flux line where the present data may be compared with previous theoretical results.[1-5] A detailed comparison to the approximate Green's-function solution of Kramer and Pesch for the low-lying energy levels[4] is reported in the Appendix. For finite flux-line distance the sharp energy levels (bound states) found for the isolated vortex become energy bands of finite width, and the wave functions of the excitations in neighboring Wigner-Seitz (WS) cells begin to overlap. The latter effect implies tunneling of quasiparticles through the vortex lattice.[19] In addition, we find situations where no scattering states exist in a finite-energy interval above $|\psi_{\rm BCS}|$. In all calculations Ginzburg-Landau (GL) parameters κ corresponding to clean Nb or V have been chosen. This allows us to answer the previously raised question concerning these materials. On the other hand, the general features of the computed energy spectrum will not depend on this par-

ticular choice of κ.

In the final section, Sec. IV, the results are summarized and some brief comments on the experimental situation are given. The recent scanning-tunneling-microscope measurements[17] of the local density of states near an isolated flux line are discussed in the light of the present numerical data.

II. METHOD OF SOLUTION

In Ref. 14 the quasiclassical equations of superconductivity have been solved, without approximations, on a hexagonal vortex lattice. The quasiclassical equations or Eilenberger equations consist of the transportlike differential equations

$$\{-iz+\mathbf{k}[\nabla-i\mathbf{a}(\mathbf{r})]\}f(z,\mathbf{k},\mathbf{r})=\psi(\mathbf{r})g(z,\mathbf{k},\mathbf{r}) , \quad (1)$$

$$\{-iz-\mathbf{k}[\nabla+i\mathbf{a}(\mathbf{r})]\}f^{+}(z,\mathbf{k},\mathbf{r})=\psi^{*}(\mathbf{r})g(z,\mathbf{k},\mathbf{r}) , \quad (2)$$

$$2\mathbf{k}\nabla g(z,\mathbf{k},\mathbf{r})=\psi^{*}(\mathbf{r})f(z,\mathbf{k},\mathbf{r})-\psi(\mathbf{r})f^{+}(z,\mathbf{k},\mathbf{r}) , \quad (3)$$

$$g=(1-ff^{+})^{1/2}, \quad \mathrm{Im}z\,\mathrm{Re}g>0 , \quad (4)$$

for the Green's functions f,f^{+},g and the self-consistency conditions (see, e.g., Ref. 14) for the potentials. The notation and system of units of Ref. 14 is used throughout the present paper.

We want to calculate the local, $\mathbf{k}$-dependent density of states, defined by

$$N(E,\mathbf{k},\mathbf{r})=\mathrm{Re}g(z,\mathbf{k},\mathbf{r}), \quad z=E+i\delta .$$

Here, δ is a positive infinitesimal quantity. Therefore, in contrast to previous work,[14] where the quasiclassical equations have been solved for purely imaginary values of $z,z=i\omega_l$ (ω_l Matsubara frequencies) the present task requires a solution of Eqs. (1)–(4) for real values of z. There are two possible ways of proceeding. N could be obtained either by analytical continuation of the Green's functions results found in Ref. 14 or by using only the previously obtained potentials $\psi,\mathbf{a}$ and solving Eqs. (1)–(4) for imaginary z. The latter strategy employed previously by Watts-Tobin *et al.* in their dirty limit calculations[20] was also chosen in the present work and turned out to be successful.

The density of states defined earlier in terms of a quasiclassical Green's function may be obtained from the spectral weight function of Gorkov's theory[21] by integrating the latter with respect to $\xi=\hbar v_F(k-k_F)$. For the homogeneous superconducting state one obtains from Eqs. (1)–(4) the well-known result

$$N(E,\mathbf{k},\mathbf{r})=\begin{cases}E/(E^2-|\psi_{\mathrm{BCS}}|^2)^{1/2}, & E>|\psi_{\mathrm{BCS}}|\\ 0, & E<|\psi_{\mathrm{BCS}}| .\end{cases} \quad (5)$$

In the next section the drastic deviations from Eq. (5) caused by the presence of flux lines will be discussed.

In this paper as well as in Ref. 14 the symmetry relations of the quasiclassical variables are extensively used in order to simplify calculations and save computer time. As can easily be shown, the relations found in Ref. 14 for real $-iz$ ($-iz=\omega_l$ in Ref. 14) remain valid for arbitrary complex-valued $-iz$ if in all complex conjugate variables the argument $-iz$ is replaced by $(-iz)^{*}$.

The symmetry relations may be used to reveal some general features of the expected results. We introduce the spatial variables $r_{\parallel}$ and $r_{\perp}$ frequently used in vortex problems. These are the coordinates[14] of a point measured with respect to unit vectors parallel and perpendicular to the considered direction $\hat{\mathbf{k}}$. The quasiparticle direction $\mathbf{k}$ will be denoted by $\mathbf{k}=(\cos\theta,\hat{\mathbf{k}})$, where $\pi/2-\theta$ is the angle between $\mathbf{k}$ and the magnetic field $\mathbf{B}=B(x,y)\mathbf{e}_z$, and the unit vector $\hat{\mathbf{k}}$ is parallel to the projection of $\mathbf{k}$ onto the xy plane.

First we note that the general result[22] that a finite density of states implies a discontinuity of $\mathrm{Re}g(E+i\delta)$ at $\delta=0$, is, in the present context, a consequence of the symmetry properties[14] of the Green's function g. Consideration of the transport equations shows that essentially two different possibilities exist for the behavior of f,f^{+},g at $\delta=0$: (i) f,f^{+},g are continuous at $\delta=0$. This implies $\mathrm{Re}g=0$ and $f=f^{+*}$ and (ii) f,f^{+},g have a discontinuity of the kind $g(0^{+})=-g(0^{-})$ at $\delta=0$. This implies $\mathrm{Im}g=0$ and $f=-f^{+*}$.

Depending on the possibility chosen, the normal Green's function g is either given by $g=(1-|f|^2)^{1/2}$, $|f|^2>1$ [in case (i)], or by $g=(1+|f|^2)^{1/2}$ [in case (ii)]. If we assume f and g to be continuous functions of the variable $r_{\parallel}$, there can be no "mixing" of possibilities (i) and (ii) for a fixed value of $r_{\perp}$. The numerical results for small δ show in fact, that, for each particular value of $r_{\perp}$, either $\mathrm{Re}g=0$, $\mathrm{Im}g\neq0$, or $\mathrm{Re}g\neq0$, $\mathrm{Im}g=0$.

Consideration of the well-known local solutions of the transport equations gives some further information on the results for small $\cos\theta$. We introduce the minimal and maximal values of the order parameter modulus,

$$|\psi^{\min}(r_{\perp})|=|\psi(r_{\perp},r_{\parallel}=0)|$$

and

$$|\psi^{\max}(r_{\perp})|=\max_{\{r_{\parallel}\}}|\psi(r_{\perp},r_{\parallel})| ,$$

for a given value of $r_{\perp}$ (and $\hat{\mathbf{k}}$). Then, for small $\cos\theta$, one expects $\mathrm{Re}g(E,r_{\parallel},r_{\perp})=0$ for all $r_{\perp}$ fulfilling $E<|\psi^{\min}(r_{\perp})|$, while $\mathrm{Re}g(E,r_{\parallel},r_{\perp})\neq0$ for $E>|\psi^{\max}(r_{\perp})|$ (scattering solutions). These features are again in agreement with the numerical results. On the other hand, for

$$|\psi^{\min}(r_{\perp})|<E<|\psi^{\max}(r_{\perp})|$$

the local solutions become meaningless, since they imply a mixing of possibilities (i) and (ii). Finally, combining the above "nonmixing condition" with symmetry properties one concludes that $\mathrm{Re}g\neq0$ for $E=0$, $r_{\perp}=0$ and arbitrary values of $\mathbf{k}$. Thus, at $E=0$ single-particle excitations of any direction exist at the vortex center. This completes our listing of general features of the expected results.

Two different methods of solving Eqs. (1)–(4) for imaginary z have been used alternatively in Ref. 14, the "explosion method," and the "symmetry method." It turns out that both of these methods may still be applied, after appropriate modifications, to the present problem. This is to be expected for the symmetry method which rests entirely on properties independent of z but is not so clear

for the explosion method.

The characteristic length for the spatial variation of the Green's functions is the coherence length, or explosion length $\bar{\xi}_G$ defined in Ref. 14. If z changes from imaginary to real values, $\bar{\xi}_G$ becomes a complex-valued quantity and the following two modifications in the behavior of the Green's functions occur: First, the explosion becomes "slower," i.e., the actual explosion length increases. Second, the numerical solutions show rather strong spatial oscillations in addition to the exponentially increasing behavior which is the dominating one for imaginary z. Nevertheless the explosion method may still be used successfully. However, the range of parameters $\mathbf{k},E$, where it can be applied, becomes strongly reduced and the oscillating behavior of the Green's functions leads to additional complications in the numerical calculations. Solving the transport equations for real energies requires, generally, a much larger numerical effort as compared to the previous case of imaginary energies. This is due to the sharp structures which occur in the density of states (see the next section), in particular in the low-energy range. In this paper we restrict ourselves to a discussion of the local, $\mathbf{k}$-dependent density of states. A calculation of densities of states averaged with respect to $\mathbf{r}$ and $\mathbf{k}$ will be a subject of future research.

III. RESULTS AND DISCUSSION

The following notation will be used in this section. For the greater part of the discussion following it will be convenient to represent the density of states in terms of the spatial variables (Ref. 14) $r_\parallel$ and $r_\perp$. For computational reasons only "rational" values of $\hat{\mathbf{k}}$, defined by

$$\hat{\mathbf{k}}_{n,m}=(n\mathbf{r}_1+m\mathbf{r}_2)/|n\mathbf{r}_1+m\mathbf{r}_2|$$

will be used (n,m are integers, $\mathbf{r}_1$ and $\mathbf{r}_2$ are the elementary translations of the hexagonal vortex lattice[14]). Thus the density of states will be written as

$$N(E,\mathbf{k},\mathbf{r})=N(E,\cos\theta,\hat{\mathbf{k}}_{n,m},\mathbf{r}) .$$

In addition to these parameters, it depends on reduced temperature $t=T/T_c$, Ginzburg-Landau parameter of the clean material κ, and equilibrium flux-line distance d [or macroscopic induction $\bar{B}=4\pi/(d^2\sqrt{3})$]. The latter set of parameters enters the transport equations implicitly via the self-consistent potentials $\psi,\mathbf{a}$, which were computed in a previous work.[14]

The parameters and potentials used in this paper correspond to actually existing clean type-II superconductors like Nb ($\kappa=0.72$) and V ($\kappa=0.8$). In the following discussion emphasis is placed on the region of large (or intermediate) flux-line distance and low energy where the density of states shows its most abrupt spatial variations.

A. Large flux-line distance

In the limit of large flux-line distance, $d\to\infty$, the density of states becomes invariant under simultaneous rotations of $\mathbf{r}$ and $\hat{\mathbf{k}}$. To distinguish this situation from that of finite d the $\hat{\mathbf{k}}$-dependent coordinates $r_\parallel,r_\perp$ will be denoted by x,y in this section.

Let us first consider the bound states occurring in the energy range $E<|\psi_{\mathrm{BCS}}|$. A typical numerical result is shown in Fig. 1. (In all figures showing the spatial variation of N only one Wigner-Seitz cell is displayed. To make the latter visible it has been elevated relative to the physically meaningless region outside it. The zero point of N is where the perpendicular axis cuts the plane of the WS cell.) One finds that N considered as a function of x,y vanishes everywhere except on a straight line $y=\mathrm{const}=y(E)$. This straight line, being parallel to the projection of the specified direction $\mathbf{k}$ onto the x,y plane, may be considered as the projected spatial region accessible to a quasiparticle of energy E (measured with respect to the Fermi energy) and momentum $\hbar k_F\mathbf{k}$. It will frequently be referred to as "quasiparticle path" in what follows. The bounded motion of the quasiparticles may be considered as a consequence of Andreev reflection at the order-parameter potential wall. Along the line $y=y(E)$, N has a single maximum at $x=0$ and vanishes for $x=\pm\infty$. The shortest distance $y(E)$ of the quasiparticle path from the vortex axis is a monotonically increasing function of E (see following). For $E=0$ the line position is given by $y=0$; i.e., the lowest excitations cut the vortex center. With decreasing angle $\pi/2-\theta$ between $\mathbf{k}$ and $\mathbf{e}_z$ the region of nonzero N, centered around $x=0$, becomes smaller and the maximal value of N strongly increases. For $E=0$ and $\cos\theta=1$ the region of nonzero N defines something like a "range of the gapless regime," which is of the order of a few coherence lengths ξ_{BCS}. Only one bound state has been found for fixed values of $\mathbf{k}$ and $\mathbf{r}$ (however, the smallest θ used in the calculations was given by $\cos\theta=0.36$).

For a really isolated flux line the density of states is a discontinuous function[4] of y with a singularity at $y=y(E)$. Of course, in actual numerical calculations a finite flux-line distance must be used yielding quasiparticle paths of finite width Δy and a finite magnitude of N. The properties discussed earlier may, however, easily be derived from the asymptotic behavior of the numerical results.

These results qualitatively agree with the low-lying ex-

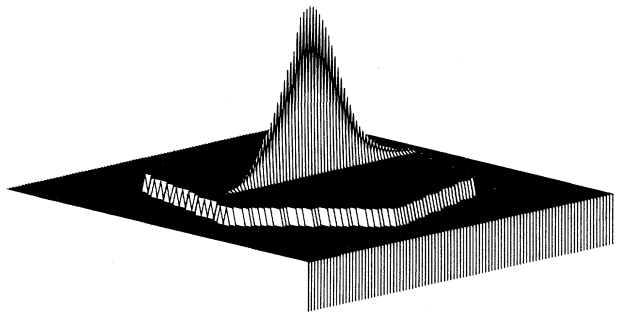

FIG. 1. Spatial variation of the density of states $N(E,\cos\theta,\hat{\mathbf{k}},\mathbf{r})$ for $E=0$, $\cos\theta=0.36$, $\hat{\mathbf{k}}=\hat{\mathbf{k}}_{31}$ in a WS cell. N is only different from zero on the line $r_\perp=0$; its maximal value is 2.5×10^2. Further parameters used in this plot are $\kappa=0.72$, $T/T_c=0.6$, and $d=7.5\xi_{\mathrm{BCS}}$.

citations of an isolated vortex first found by Caroli *et al.*[1] for $x \gg 1$ and subsequently studied for arbitrary values of κ by Bardeen *et al.*[3] These authors did not employ the quasiclassical approximation and used a set of quantum numbers different from the present one. The results of Caroli *et al.*[1] for $E \ll |\psi_{\rm BCS}|$ may be compared with the present ones by identifying their quantum number μ with the z component of the classical angular momentum of the quasiparticle, i.e., replacing $\hbar\mu$ by $\hbar y k_F \cos\theta$. In the framework of the quasiclassical Green's function method the low-lying states were studied by Kramer and Pesch.[4,5] In the Appendix we review the relevant parts of their theory and calculate an analytical expression [Eq. (A12)] for $y(E)$ which agrees fairly well with the present numerical results.

For small $\cos\theta$ the low-lying energy levels are, according to the numerical data, given by

$$E(y)=\mathrm{sgn}(y)|\psi(0,y)| \ . \tag{6}$$

An interesting result of the numerical work is that Eq. (6) presents a fairly good approximation of the data for arbitrary values of $\cos\theta$. The maximal deviation from Eq. (6)—for $\cos\theta=1$—is lower than 10% as shown in Fig. 2. Thus the main contribution to $E(y)$ stems from the minimum value of the self-consistently determined order parameter on the considered path $y=$const. This result is in contrast to Ref. 3, where it was claimed that for $\kappa \simeq 1$ the energy levels are given by two contributions of comparable magnitude, one stemming from the order parameter and one from the magnetic field.

Equation (6) agrees exactly with the corresponding result of the Kramer-Pesch approximation reported in the Appendix. As is further discussed in the Appendix $E(y)$ is, for arbitrary $\cos\theta$, determined by the values of order parameter, superfluid velocity, and the derivatives of these quantities at $x=0$. It turns out that the singular part of the superfluid velocity is canceled by the first derivative of the order parameter (see the Appendix) and

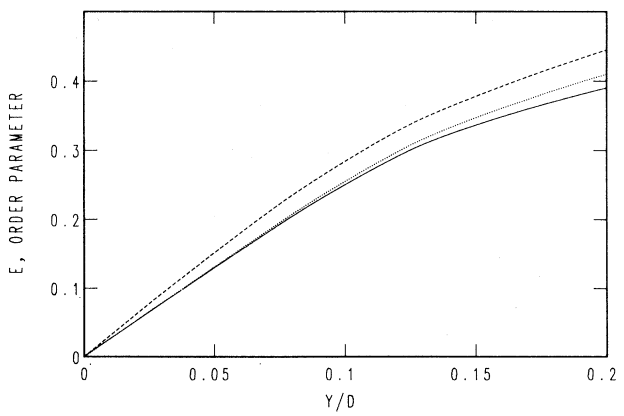

FIG. 2. Comparison of the minimum value of the order parameter modulus $|\psi(0,y)|$ (solid line) with the energy levels $E(y)$ for $\cos\theta=0.36$ (dotted line) and for $\cos\theta=0.97$ (dashed line). Parameters used in this plot are $\kappa=0.72$, $T/T_c=0.6$, and $d=7.5\xi_{\rm BCS}$. The result for $\cos\theta=0.97$ has been corrected for (small) effects of finite d.

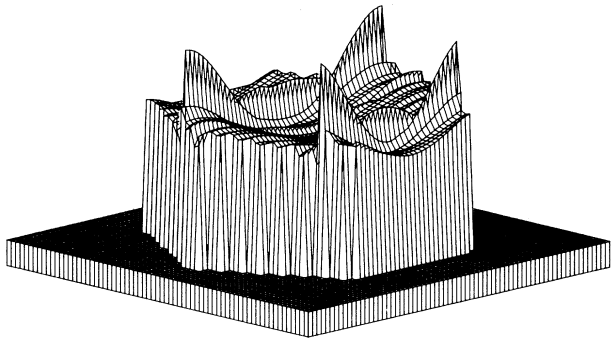

FIG. 3. Spatial variation of the density of states $N(E,\cos\theta,\hat{\mathbf{k}},\mathbf{r})$ for $E=2\psi_{\rm BCS}$, $\cos\theta=0.97$, and $\hat{\mathbf{k}}=\hat{\mathbf{k}}_{11}$ in a WS cell. The maximal value of N is 2.15. Further parameters used in this plot are $\kappa=0.72$, $T/T_c=0.6$, and $d=7.5\xi_{\rm BCS}$.

all other correction terms due to the finite $\cos\theta$ have a relatively small influence on the final result.

An "excitation threshold" as given by Eq. (6) has been predicted by de Gennes[23] considering a situation where magnetic field effects can be neglected. Our results show that the low-lying energy levels of a dilute vortex lattice are approximately given by this threshold value. For higher values of κ than the present ones one expects even smaller deviations from Eq. (6).

At higher energies $E/\psi_{\rm BCS} \cong 1$, scattering states appear at the boundary of the WS cell and the line structure starts to break down. At still higher energies ($E/\psi_{\rm BCS} > 1.5$) these scattering states extend in a more or less isotropic manner over the whole space. The density of states plotted in Fig. 3 is mainly isotropic. In addition, it shows some vestiges of a $\hat{\mathbf{k}}$-dependent behavior of N. The latter is a consequence of flux-line interactions.

B. Intermediate flux-line distance

In this section we consider a range of low but finite inductions, to be realized in the vicinity of the lower critical field H_{c1}, and discuss how the excitations of the isolat-

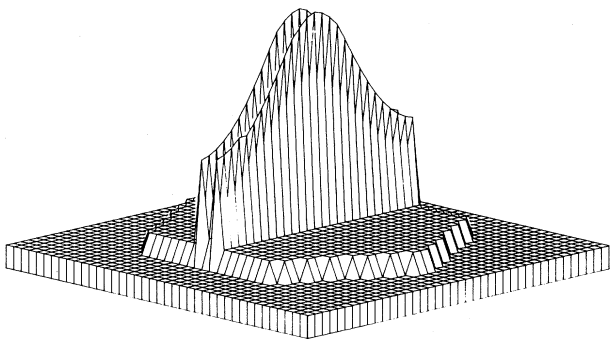

FIG. 4. Spatial variation of the density of states $N(E,\cos\theta,\hat{\mathbf{k}},\mathbf{r})$ for $E=0$, $\cos\theta=0.97$, and $\hat{\mathbf{k}}=\hat{\mathbf{k}}_{10}$ in a WS cell. The vector $\hat{\mathbf{k}}$ defines the preferred direction (parallel to the $r_{\|}$ axis) in this diagram. The maximal value of N is 4.8. Further parameters used in this plot are $\kappa=0.72$, $T/T_c=0.6$, and $d=7.5\xi_{\rm BCS}$.

ed vortex are modified by (small) flux-line interactions. Essentially two things happen: First, the sharp lines of the isolated vortex at low energy split into a double-peak structure of finite width $\Delta r_\perp(d)$, as shown in Fig. 4. In the Appendix an estimate for $\Delta r_\perp(d)$ and the corresponding width of the energy levels $\Delta E(d)$ is given which agrees fairly well with the present results. For the low inductions considered here the relation $\Delta r_\perp(d) \ll d$ still holds, so the line shaped structure of the excitations is preserved.

The second modification brought about by the finite flux-line distance (also shown in Fig. 4) is an increased extension of the wave functions in $r_\parallel$ direction, i.e., an increase of what has been called earlier the range of the gapless regime. If the wave function is nonzero at the boundary of the WS cell, the former bound state of the isolated vortex has changed into a tunneling state. The latter represents a single-particle excitation which extends over the whole flux-line lattice. These effects lie outside the range of validity of the Kramer-Pesch approximation where wave functions describing independent flux lines are used. Tunneling states of quasiparticles in a periodic vortex lattice have however been predicted by Canel.[19] He showed that these excitations should behave like Bloch electrons in a magnetic field, without evaluating their wave functions explicitly.

A quasiparticle trajectory of direction $\hat{\mathbf{k}}_{n,m}$ connecting a starting point $\mathbf{r}_A$ with its translational-equivalent end point $\mathbf{r}_E$ ($\mathbf{r}_E = T_{n,m}\mathbf{r}_A$, the operator $T_{n,m}$ is defined in Ref. 14) consists of several segments corresponding to the different WS cells on this path. Translational invariance implies that the behavior of the density of states in all these segments is reproduced in the original WS cell. Therefore, for small E, one expects $N(E,\mathbf{k},\mathbf{r})$ to be different from zero on several straight lines which are all equivalent in the sense that each one passes through a flux-line center (at $E=0$). The present results for a hexagonal vortex lattice show indeed the expected structure (see Figs. 4 and 5–7).

In actually existing clean type-II superconductors like Nb or V the maximal flux-line distance is limited by flux-line attraction.[11,14] A lower bound for the influence of tunneling on the mixed state of these materials may be obtained by considering an induction $\bar{B} < B_0$, where B_0 is the discontinuous jump of the induction at the lower critical field H_{c1}. Figures 4 and 7 show our results for such a situation. The parameters used in Figs. 4 and 7 are $E=0$, $\cos\theta \cong 1$ (maximal tunneling), and $\hat{\mathbf{k}}_{10}, \hat{\mathbf{k}}_{11}$ (the two simplest directions). Already at these low inductions, corresponding to a flux-line distance of about $8\xi_{\mathrm{BCS}}$ a considerable overlap of wave functions in neighboring WS cells occurs. Considering the totality of possible quasiparticle directions, one is led to the conclusion that the mixed state of pure Nb and V is gapless everywhere. This result holds for arbitrary $\bar{B}$ and T with the possible exception of a small region near T_c where no flux-line attraction exists and d may become arbitrarily large. Of course, near T_c the order-parameter itself is strongly suppressed. Clearly, in the mixed state the tunneling character of the quasiparticle motion becomes even stronger. Figures 5 and 6 refer to a situation near H_{c1} and a "less rational" direction $\hat{\mathbf{k}}_{31}$. Comparison of Figs. 5

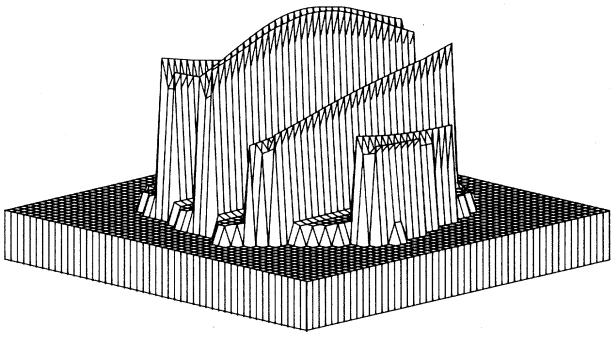

FIG. 6. Spatial variation of the density of states $N(E,\cos\theta,\hat{\mathbf{k}},\mathbf{r})$ for $E=0$, $\cos\theta=0.97$, and $\hat{\mathbf{k}}=\hat{\mathbf{k}}_{31}$ in a WS cell. The vector $\hat{\mathbf{k}}$ defines the preferred direction (parallel to the $r_\parallel$ axis) in this diagram. The maximal value of N is 2.7. Further parameters used in this plot are $\kappa=0.8$, $T/T_c=0.5$, and $d=3.4\xi_{\mathrm{BCS}}$.

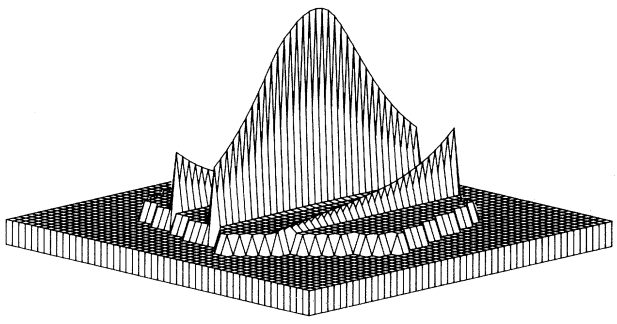

FIG. 5. Spatial variation of the density of states $N(E,\cos\theta,\hat{\mathbf{k}},\mathbf{r})$ for $E=0.15\psi_{\mathrm{BCS}}$, $\cos\theta=0.75$, and $\hat{\mathbf{k}}=\hat{\mathbf{k}}_{31}$ in a WS cell. The vector $\hat{\mathbf{k}}$ defines the preferred direction (parallel to the $r_\parallel$ axis) in this diagram. The maximal value of N is 8.7. Further parameters used in this plot are $\kappa=0.8$, $T/T_c=0.5$, and $d=5.3\xi_{\mathrm{BCS}}$.

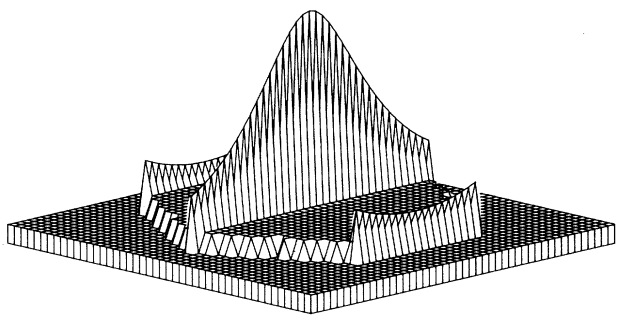

FIG. 7. Spatial variation of the density of states $N(E,\cos\theta,\hat{\mathbf{k}},\mathbf{r})$ for $E=0$, $\cos\theta=0.97$, and $\hat{\mathbf{k}}=\hat{\mathbf{k}}_{11}$ in a WS cell. The vector $\hat{\mathbf{k}}$ defines the preferred direction (parallel to the $r_\parallel$ axis) in this diagram. The maximal value of N is 10.2. Further parameters used in this plot are $\kappa=0.72$, $T/T_c=0.6$, and $d=7.5\xi_{\mathrm{BCS}}$.

and 6 illustrates the decrease in tunneling with increasing d and decreasing angle between $\mathbf{k}$ and the vortex axis.

Of course, each individual quasiparticle state of momentum $\mathbf{k}$ at a particular point $\mathbf{r}$ may have one or several gaps in its energy spectrum depending on the chosen values of $\mathbf{r}$ and $\hat{\mathbf{k}}$. We restrict ourselves to a discussion of the local energy spectrum at the flux-line center, which is of particular interest. Figure 8 shows $N(E,\mathbf{k},\mathbf{r})$ at $\mathbf{r}=0$ for $\cos\theta\cong 1$, and $\hat{\mathbf{k}}=\hat{\mathbf{k}}_{10}$. Here again parameters corresponding to $\bar{B}<B_0$ have been chosen (for the same reasons as discussed in the context of Figs. 4 and 7). Besides the line splitting and broadening of the single-particle excitations at low energy which was discussed earlier, one notices in Fig. 8 a significant reduction of the scattering states at $E/\psi_{\rm BCS}\gtrsim 1$. These two effects are related to each other by the sum rule

$$\int_0^\infty dE[N(E,\mathbf{k},\mathbf{r})-1]=0\ ,$$

which requires a reduction of the high-energy states as a consequence of the increased weight at low energies. For an isolated flux-line scattering states appear for $E/\psi_{\rm BCS}>1$ with a divergent behavior of the density of states[24] at the band edge $E=\psi_{\rm BCS}$. Figure 8 shows that the reduction of states brought about by the vortex interaction takes place in such a way that part of the spectrum near $E=\psi_{\rm BCS}$ is eliminated and consecutively the band edge is shifted to higher energies and smeared out. A second example for $N(E,\mathbf{k},0)$ is plotted in Fig. 9 where $\mathbf{k}=(0.97,\hat{\mathbf{k}}_{31})$ and parameters corresponding to a situation near H_{c1} have been chosen. For this less rational direction and relatively high induction a broad tunneling state appears leading to two gaps at the vortex center.

We should mention that, in the present work, more emphasis is placed upon general properties of the energy spectrum than upon quantitative details. In particular, no attempt has been made to resolve the details of the peak structure in Figs. 8 and 9 by means of enhanced numerical effort. Similar remarks apply to the graphs showing the space dependence of the density of states. Use of

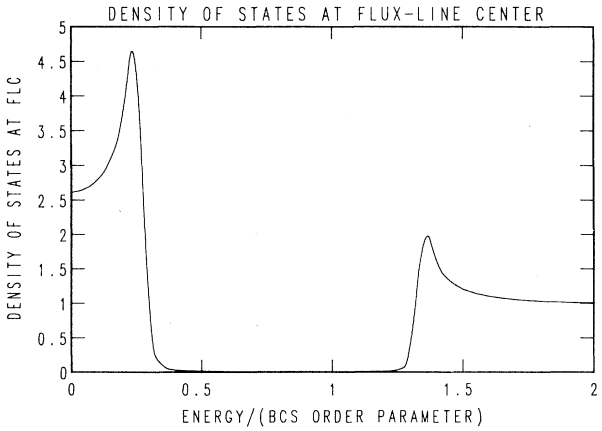

FIG. 8. Energy dependence of the density of states $N(E,\cos\theta,\hat{\mathbf{k}},\mathbf{r})$ for $\cos\theta=0.97$ and $\hat{\mathbf{k}}=\hat{\mathbf{k}}_{10}$ at the flux-line center $\mathbf{r}=0$. Further parameters used in this figure are $\kappa=0.72$, $T/T_c=0.6$, and $d=7.5\xi_{\rm BCS}$.

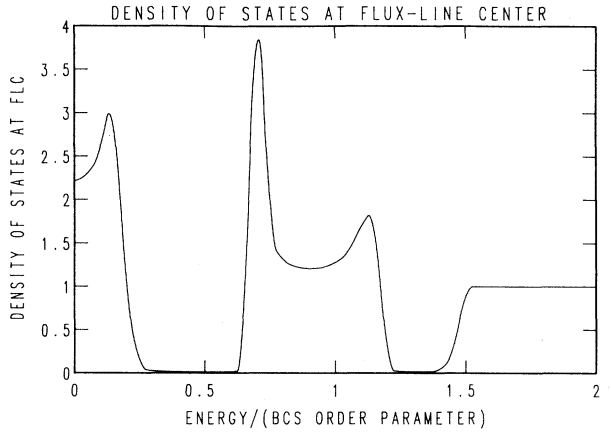

FIG. 9. Energy dependence of the density of states $N(E,\cos\theta,\hat{\mathbf{k}},\mathbf{r})$ for $\cos\theta=0.97$ and $\hat{\mathbf{k}}=\hat{\mathbf{k}}_{31}$ at the flux-line center $\mathbf{r}=0$. Further parameters used in this figure are $\kappa=0.8$, $T/T_c=0.5$, and $d=3.4\xi_{\rm BCS}$.

enlarged computer capacities may lead to small deviations from the present results without changing the qualitative conclusions drawn in this paper.

Obviously, the deficit of states near $E=\psi_{\rm BCS}$ shown in Figs. 8 and 9 is not restricted to the flux-line center but occurs in a large part of the WS cell. Therefore, the tunneling processes will lead to a strong overall reduction of the states available near $E\sim\psi_{\rm BCS}$. (We should mention that a similar, but much smaller, reduction of states will also occur for an isolated flux line.) This result is consistent with ultrasonic attenuation data[25] on Nb indicating the inadequacy of independent flux-line theories.

C. Small flux-line distance

Only a few calculations have been performed in the induction range close to H_{c2}. A typical result is shown in Fig. 10 where $N(0,0.97,\hat{\mathbf{k}}_{10},\mathbf{r})$ for $\bar{B}/H_{c2}=0.74$ is plotted. As expected, at this high induction the line-shaped structure of the density of states no longer exists. The re-

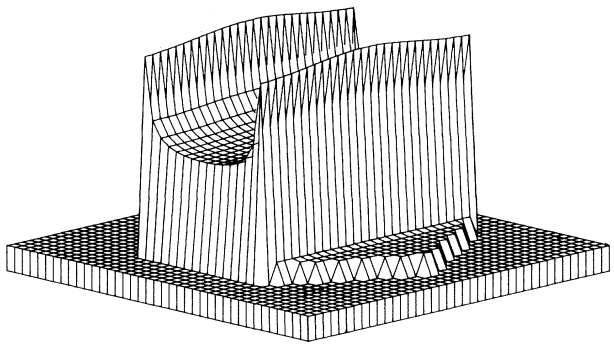

FIG. 10. Spatial variation of the density of states $N(E,\cos\theta,\hat{\mathbf{k}},\mathbf{r})$ for $E=0$, $\cos\theta=0.97$, and $\hat{\mathbf{k}}=\hat{\mathbf{k}}_{10}$ in a WS cell. The vector $\hat{\mathbf{k}}$ defines the preferred direction (parallel to the $r_{\|}$ axis) in this diagram. The maximal value of N is 2.2. Further parameters used in this plot are $\kappa=0.8$, $T/T_c=0.5$, and $d=3.4\xi_{\rm BCS}$.

gion of nonvanishing N extends over most of the space, while the double peak structure discussed in Sec. III B is still visible. The results shown in Figs. 10 and 6 have been produced using the same set of parameters, except for the quasiparticle direction $\hat{\mathbf{k}}$. For the direction $\hat{\mathbf{k}}_{31}$, considered in Fig. 6, several energy bands of relatively small width occur (at each space point), while $\hat{\mathbf{k}}_{10}$, considered in Fig. 10, leads to a single band of great width. The general trend of increased pairbreaking with increasing induction shows up in the present context as an increase of the spatial extension of the wave functions in both the $r_{\parallel}$ and the $r_{\perp}$ direction.

IV. CONCLUDING REMARKS

The local, direction-resolved density of states in the vortex state of clean type-II superconductors has been calculated self-consistently. This numerical study has been performed in the framework of the quasiclassical formulation (in its isotropic, weak-coupling version) of the microscopic theory of superconductivity. No approximations have been made apart from standard approximations in numerical routines. Material parameters corresponding to clean Nb or V have been chosen.

The energy spectrum of a vortex lattice has been obtained for arbitrary energies and inductions, and the tunneling states of quasiparticles have been calculated. A shift of continuum states to energies higher than $|\psi_{\mathrm{BCS}}|$ has been found as a consequence of flux-line interactions. Besides that, some conclusions specific to the important materials Nb and V may be drawn. Transport phenomena at low inductions are usually analyzed in terms of the following two kinds of elementary excitations of an isolated vortex: bound states which are confined to the vortex core, and unbound states which become BCS quasiparticles far from the core. The present results provide evidence, from a theoretical point of view, that both of these concepts become more or less useless for a description of transport processes in actually existing clean type-II superconductors like Nb and V. This is a consequence of strong tunneling processes which dominate the excitation spectrum already at the lowest possible inductions, near the first-order transition at H_{c1}. Jump and Gough[26] and Muirhead and Vinen[27] arrived at a similar conclusion by comparing predictions of independent flux-line theories[7] with experimental data on ultrasonic attenuation[26] and thermal conductivity[27] in Nb (see also the detailed discussion in Ref. 25). The present results may only be considered as a first step towards a quantitative explanation of the observed deviations from the isolated vortex behavior, since, despite several promising attempts,[28,29] a complete theory of transport phenomena in a dense vortex lattice has not been worked out up to now.

Finally, we shall comment on recent tunneling experiments[17] providing information on the local density of states near a single flux line. The quantity dI/dV observed in these experiments is a weighted average of the direction-resolved tunneling conductance $\sigma(V,\mathbf{k},\mathbf{r})$. One may assume that the observed dI/dV agrees qualitatively, with respect to its dependence on voltage V and position $\mathbf{r}$, with the tunneling conductance $\sigma(V,\mathbf{r})$. The latter is defined as the convolution of $N(E,\mathbf{r})$ and the derivative of the Fermi distribution function.

In Ref. 17 the voltage dependence of the local conductance $\sigma(V,\mathbf{r})$ has been measured for different values of the radial distance from the vortex center r. From the previously discussed theoretical results, like those presented in Fig. 8, the qualitative behavior of $N(E,r)$ and $\sigma(E,r)$, for an isolated flux line can easily be deduced. Generally, one finds that, in the bound-state region and for a given value of r, contributions to $N(E,r)$ can only occur in an energy range $E \leq E_0 \cong |\psi(r)|$, while continuum states will occur for $E > E_c$, where E_c depends weakly on r and is approximately given by $|\psi_{\mathrm{BCS}}|$. In particular, at the flux-line center, $r=0, N(E,0)$ has a sharp peak at $E=0$ (compare Fig. 8). This result may also be derived from the theory of Kramer and Pesch. In the tunneling conductance $\sigma(V,r)$ this peak will also appear, at $V=0$, but with a finite, temperature-dependent width. This behavior is in agreement with the data reported in Ref. 17. The same applies to the observed broadening of the peaks with decreasing vortex distance (see Sec. III B).

Thus, theory predicts, in agreement with experimental data[17] but in disagreement with some previous statements in the theoretical literature,[30] that the energy dependence of the local density of states at $r=0$ is (in the clean limit) very different from the normal-state behavior. We note that the energy spectrum depends on the order parameter in a nonlocal way and that the commonly used concept of Caroli *et al.*[1] of a "normal core radius" of the order of the coherence length refers to the total density of states rather than to the local one. Work is in progress in order to explain the experimental results of Ref. 17 in a more quantitative way.

ACKNOWLEDGMENTS

I am deeply indebted to L. Kramer, W. Pesch, and D. Rainer for many stimulating discussions and helpful comments. This work was supported by the Liuzer Hochschulfouds.

APPENDIX

In this appendix we review the approximate calculation[4] by Kramer and Pesch of the low-lying excitations in a dilute vortex lattice and calculate analytical expressions for the energy levels in two simple cases.

Following Kramer and Pesch we formally eliminate the vector potential from Eqs. (1)–(4) by means of a gauge transformation

$$\psi=\bar{\psi}e^{i\tilde{\theta}},\quad f=\bar{f}e^{i\tilde{\theta}},\quad f^{+}=\bar{f}^{+}e^{-i\tilde{\theta}},$$

$$\tilde{\theta}(r_{\parallel},r_{\perp},\phi_k)=\int_0^{r_{\parallel}}\hat{\mathbf{k}}\mathbf{a}(r'_{\parallel},r_{\perp},\phi_k)dr'_{\parallel}+\phi_k\ .$$

Here, ϕ_k denotes the angle between $\hat{\mathbf{k}}$ and the x axis. For $\phi_k=0$ ($\hat{\mathbf{k}}=\hat{\mathbf{k}}_{10}$), the following symmetry relations may be derived:

$$\bar{\psi}(-r_{\parallel})=-\bar{\psi}^{*}(r_{\parallel}),$$

$$\bar{f}(-r_{\parallel})=-\bar{f}^{+}(r_{\parallel}),$$

$$g(r_{\parallel})=g(-r_{\parallel}),$$

and the transport equations take the form

$$\left[-iz+\cos\theta\frac{\partial}{\partial r_\parallel}\right]\bar{f}(r_\parallel)=\bar{\psi}g(r_\parallel)\ , \tag{A1}$$

$$2\cos\theta\frac{\partial}{\partial r_\parallel}g(r_\parallel)=\bar{\psi}^*\bar{f}(r_\parallel)+\bar{\psi}\bar{f}(-r_\parallel)\ , \tag{A2}$$

$$g(r_\parallel)=[1+\bar{f}(r_\parallel)\bar{f}(-r_\parallel)]^{1/2},\quad \mathrm{Im}z\,\mathrm{Reg}(r_\parallel)>0\ . \tag{A3}$$

A similar set of simplified equations may be derived for two other high-symmetry directions, $\hat{\mathbf{k}}_{01}$ and $\hat{\mathbf{k}}_{11}$. For an isolated vortex Eqs. (A1)–(A3) hold for arbitrary $\hat{\mathbf{k}}$. Equations (A1)–(A3) have to be supplemented by proper boundary conditions. For an isolated vortex the solutions must agree with the Meissner-state solution at large distance from the vortex axis. For a vortex lattice of nearest-neighbor distance d, translational symmetry[14] implies the following condition:

$$\bar{f}(r_\parallel+d)=\bar{f}(r_\parallel)\exp\left[i\int_0^d dr'_\parallel\hat{\mathbf{k}}\cdot\mathbf{v}_s(r'_\parallel,r_\perp,0)\right]\ , \tag{A4}$$

where $\mathbf{v}_s(r_\parallel,r_\perp,\phi_k)$ is the superfluid velocity defined by $\mathbf{v}_s=\nabla\phi-\mathbf{a}$ (ϕ is the phase of the order parameter ψ).

For $E=0$ and $r_\perp=0$ Eqs. (A1)–(A3) have been solved exactly[4] by Kramer and Pesch. Using this solution as a starting point these authors derived an approximate expression for g, valid in the range of small $r_\parallel$, small $r_\perp$, and large d. In terms of s and a, the symmetric and antisymmetric parts of $\bar{f}$, this solution reads

$$g=(1+s^2-a^2)^{1/2}\ , \tag{A5}$$

$$s(r_\parallel,r_\perp)=Ae^{-u(r_\parallel,r_\perp)}\ , \tag{A6}$$

$$a(r_\parallel,r_\perp)=\frac{A}{\cos\theta}\int_0^{r_\parallel}dr'_\parallel[-\delta-iE+i|\psi(r'_\parallel,r_\perp)|\sin\Omega(r'_\parallel,r_\perp)]\times e^{-u(r'_\parallel,r_\perp)}\ , \tag{A7}$$

$$u(r_\parallel,r_\perp)=\frac{1}{\cos\theta}\int_0^{r_\parallel}dr'_\parallel|\psi(r'_\parallel,r_\perp)|\cos\Omega(r'_\parallel,r_\perp)\ , \tag{A8}$$

where $\Omega=\tilde{\theta}-\phi$. An approximate form of the quantity Ω will be given below. The range of validity of Eqs. (A5)–(A8) may be extended to arbitrary $r_\parallel$ in the following way. For $r_\perp=0$, $E=0$ one has $a=0$, $g=-s$, and $A\to\infty$. Therefore, for small $r_\perp$ and large A the relation $g\cong s$ will be approximately valid for arbitrary $r_\parallel$. On the other hand, condition (A4) implies $|s|\ll|a|$, and consecutively $g\cong(1-a^2)^{1/2}$, for small $r_\perp$ and large $r_\parallel$. Equating the two apparently contradictory solutions at $r_\parallel=d/2$ yields the condition $s^2+a^2=1$, which determines the unknown amplitude A. One obtains[4]

$$A=\{e^{-2u(d/2,r_\perp)}+[(\delta-iE)\alpha(d/2,r_\perp)+iI_1(d/2,r_\perp)]^2\}^{-1/2}\ , \tag{A9}$$

where

$$\alpha(d/2,r_\perp)=\frac{1}{\cos\theta}\int_0^{d/2}dr'_\parallel e^{-u(r'_\parallel,r_\perp)}\ , \tag{A10}$$

$$I_1(d/2,r_\perp)=-\frac{1}{\cos\theta}\int_0^{d/2}dr'_\parallel|\psi(r'_\parallel,r_\perp)|\times\sin\Omega(r'_\parallel,r_\perp)e^{-u(r'_\parallel,r_\perp)}\ . \tag{A11}$$

The solution given by Eqs. (A9)–(A11) is a good approximation for large d, small $r_\perp$ (small E), and large A. The singularities of A give the positions $r_\perp(E,d)$, or alternatively the energy levels ($E=I_1/\alpha$) where sharp excitations occur in a dilute vortex lattice. These positions are calculated later for two simple cases and compared with the present numerical results.

To obtain our first estimate of the low-lying levels, we assume $\mathbf{a}\cong 0$,

$$\Omega(r_\parallel,r_\perp)\cong-\arctan\frac{r_\perp}{r_\parallel}\ ,$$

and approximate the variation of the order parameter by

$$\psi=\begin{cases}\psi_{\mathrm{BCS}}\dfrac{r}{\xi_1}, & r<\xi_1\\ \psi_{\mathrm{BCS}}, & r>\xi_1\ .\end{cases}$$

For $d\to\infty$ and $r_\perp/\xi_1\ll 1$, Eq. (A9) yields $E=E_\infty(r_\perp)$, where

$$E_\infty(r_\perp)/\psi_{\mathrm{BCS}}=(r_\perp/\xi_1)g(\psi_{\mathrm{BCS}}\xi_1/\cos\theta)\ . \tag{A12}$$

The function g is given by

$$g(x)=\frac{\sqrt{\pi x/2}\Phi(\sqrt{x/2})+xe^{x/2}E_1(x)}{\sqrt{\pi x/2}\Phi(\sqrt{x/2})+e^{-x/2}}\ , \tag{A13}$$

where Φ is the error function as defined in Ref. 31 and E_1 is an exponential integral. For finite d the sharp levels split into a double-peak structure of finite width in agreement with the results presented, e.g., in Fig. 4. The density of states differs from zero in a range

$$E_-(r_\perp,d)<E<E_+(r_\perp,d)$$

showing a singular behavior at $E=E_\pm$. The band edges $E_\pm$ are given by

$$E_\pm(r_\perp,d)=\bar{E}(r_\perp,d)\pm e^{-u(d/2,r_\perp)}\ ,$$

where

$$u(r_\parallel,r_\perp)=\frac{\psi_{\mathrm{BCS}}}{\cos\theta}\left[(r_\parallel^2+r_\perp^2)^{1/2}-\frac{\xi_1}{2}(1+r_\parallel^2/\xi_1^2)\right]\ ,$$

and (to leading order in $1/d$)

$$\bar{E}(r_\perp,d)\cong E_\infty(r_\perp)+\frac{r_\perp}{\xi_1}\psi_{\rm BCS}\frac{g(b\xi_1)e^{b(\xi_1-d)/2}}{\sqrt{\pi}(b\xi_1/2)^{1/2}\Phi[(b\xi_1/2)^{1/2}]+e^{-b\xi_1/2}}\ . \tag{A14}$$

In Eq. (A14) the abbreviation $b=\psi_{\rm BCS}/\cos\theta$ has been used. Taking an estimate for ξ_1 from the computed ψ the predictions of the Kramer-Pesch (KP) theory may be compared with the present results. Reasonable agreement is found with regard to both the level positions and the widths of the line splitting.

The second situation we shall consider is that of small $\cos\theta$, i.e., quasiparticle motion nearly parallel to the vortex axis. In this case only the isolated flux line will be considered. The preceding results of the KP theory, Eqs. (A9)–(A11) have been derived by assuming $A\gg1$, a condition which is generally not fulfilled for small $\cos\theta$. However, if we restrict ourselves to a determination of sharp energy levels, where $A\to\infty$ by definition, the Kramer-Pesch approximation may still be used for arbitrary small $\cos\theta$. In addition we should point out that this approximation in order to be valid requires the existence of an infinite path through the vortex lattice. If $\cos\theta=0$ holds exactly, such a path does not exist. Then the particle motion is restricted to a single point in the xy plane and one obtains the well-known local solutions of the transport equations which are different from the corresponding solutions of the Kramer-Pesch theory. Nevertheless, this theory may be used to calculate the energy levels for arbitrary small $\cos\theta$, provided an infinite quasiparticle path through the vortex lattice exists. The limit $\cos\theta\cong0$ is to be understood in this sense.

Evaluating the integrals in Eqs. (A10) and (A11) for $\cos\theta\cong0$ by means of a simple saddle-point method one obtains

$$E(r_\perp)=\mathrm{sgn}(r_\perp)|\psi(0,r_\perp)|\ . \tag{A15}$$

This result agrees with the first of our estimates in the appropriate limit, but does not depend on a particular model for the order parameter variation. The level positions obtained numerically agree exactly with Eq. (A15) for small $\cos\theta$ (see Fig. 2) and, on top of it, depend rather weakly on the direction of the quasiparticle momentum. As Fig. 2 shows, Eq. (A15) represents a fairly good approximation of the exact results for arbitrary values of $\cos\theta$. The weak dependence of $E(r_\perp)$ on $\cos\theta$ is also found in our first estimate given earlier [$g(x)$ is a slowly varying function].

An asymptotic expansion including higher-order terms in $\cos\theta$ may be calculated. It turns out that this asymptotic series is completely determined by the values of ψ and $\hat{\mathbf{k}}\cdot\mathbf{v}_s$ at $r_\parallel=0$ and by the derivatives of these quantities with respect to $r_\parallel$, again taken at $r_\parallel=0$. In the present notation the superfluid term is given by

$$\hat{\mathbf{k}}\cdot\mathbf{v}_s=r_\perp/r^2-(r_\perp/r)a(r)\ , \tag{A16}$$

where $r=(r_\parallel^2+r_\perp^2)^{1/2}$. The first part of Eq. (A16), stemming from the phase gradient, becomes large near the flux-line center. To see how this singular term is eliminated from the final result, the contribution of order $(\cos\theta)^1$ to $E(r_\perp)$ has been calculated. By means of asymptotic methods discussed in Ref. 32 one obtains a lengthy expression which, for small r, takes the form

$$E(r_\perp)=\mathrm{sgn}(r_\perp)\left[|\psi(0,r_\perp)|+\cos\theta\left[a(0,|r_\perp|)+\frac{\psi_3}{6\psi_1}|r_\perp|\right]\right]. \tag{A17}$$

Here, ψ_1 and ψ_3 are defined by the expansion

$$|\psi(r)|=\psi_1 r+\psi_3 r^3/6\ .$$

In the course of the calculation leading to Eq. (A17) the singular part of $\hat{\mathbf{k}}\cdot\mathbf{v}_s$ has been canceled by a term containing the first derivative of $|\psi(r)|$, which answers the previously raised question.

Eq. (A17) agrees in part with the well-known shifted energy spectrum

$$E^{\rm local}=\pm|\psi|+\hat{\mathbf{k}}\cdot\mathbf{v}_s \quad \text{at } r_\parallel=0\ ,$$

$$E^{\rm local}(r_\perp)=\mathrm{sgn}(r_\perp)\left[|\psi(0,r_\perp)|+\cos\theta\left[a(0,|r_\perp|)-\frac{1}{|r_\perp|}\right]\right].$$

The present highly nonlocal situation leads to the replacement of the singular part of $\hat{\mathbf{k}}\cdot\mathbf{v}_s$ by the last term in Eq. (A17).

[1] C. Caroli, P. G. de Gennes, and J. Matricon, Phys. Lett. **9**, 307 (1964).

[2] C. Caroli and J. Matricon, Phys. Konden. Mater. **3**, 380 (1965).

[3] J. Bardeen, R. Kümmel, A. E. Jacobs, and L. Tewordt, Phys. Rev. **187**, 556 (1969).

[4] L. Kramer and W. Pesch, Z. Phys. **269**, 59 (1974).

[5] L. Kramer, *Low Temperature Physics–LT14,* edited by M. Krusius and M. Vuorio (North-Holland, Amsterdam, 1975), Vol. 2, p. 281.

[6] M. Cyrot, Phys. Konden. Mater. **3**, 374 (1965).

[7] R. M. Cleary, Phys. Rev. B **175**, 587 (1968).

[8] K. Maki, Phys. Rev. Lett. **18**, 835 (1967).

[9] U. Brandt, W. Pesch, and L. Tewordt, Z. Phys. **201**, 209 (1967).

[10] W. Pesch, Z. Phys. B **21**, 263 (1975).

[11] L. Kramer, Z. Phys. **258**, 367 (1973); M. C. Leung and A. E. Jacobs, J. Low Temp. Phys. **11**, 395 (1973).

[12] M. Botlo, H. W. Weber, and U. Klein, *Proceedings of the 17th International Conference on Low Temperature Physics, Karlsruhe, 1984,* edited by U. Eckeru, A. Schmid, W. Weber, and H. Wühl (North-Holland, Amsterdam, 1984), Vol. 2, p.

1285.
[13]H. W. Weber and J. Rammer (unpublished).
[14]U. Klein, J. Low Temp. Phys. **69**, 1 (1987).
[15]U. Klein, L. Kramer, W. Pesch, D. Rainer, and J. Rammer (unpublished).
[16]U. Klein, J. Rammer, and W. Pesch, J. Low Temp. Phys. **66**, 55 (1987).
[17]H. F. Hess, R. B. Robinson, R. C. Dynes, J. M. Valles, and J. V. Waszczak, Phys. Rev. Lett. **62**, 214 (1989).
[18]G. Eilenberger, Z. Phys. **214**, 195 (1968).
[19]E. Canel, Phys. Lett. **16**, 101 (1965).
[20]R. Watts-Tobin, L. Kramer, and W. Pesch, J. Low Temp. Phys. **17**, 71 (1974).
[21]V. Ambegaokar, in *Superconductivity,* edited by R. D. Parks (M. Dekker, New York, 1969), Vol. 1, p. 259.
[22]P. Nozieres, *Theory of Interacting Fermi Systems,* (Benjamin, New York, 1964).
[23]P. G. de Gennes, *Superconductivity of Metals and Alloys* (Benjamin, New York, 1966), p. 155.
[24]A. L. Fetter, Phys. Rev. **A140**, 1921 (1965).
[25]W. F. Vinen, E. M. Forgan, C. E. Gough, and M. J. Hood, Physica **55**, 94 (1971).
[26]R. E. Jump and C. E. Gough, *Low Temperature Physics-LT13,* edited by K. D. Timmerhaus (Plenum, New York, 1974), Vol. 3, p. 125.
[27]C. M. Muirhead and W. F. Vinen, *Low Temperature Physics–LT13,* edited by K. D. Timmerhaus (Plenum, New York, 1974), Vol. 3, p. 130.
[28]K. Scharnberg, J. Low Temp. Phys. **6**, 51 (1972).
[29]P. Klimesch and W. Pesch, J. Low Temp. Phys. **32**, 869 (1978).
[30]R. Leadon and H. Suhl, Phys. Rev. **165**, 596 (1968).
[31]I. S. Gradshteyn and I. M. Ryzhik, *Table of Integrals, Series and Products* (Academic, New York, 1980).
[32]R. B. Dingle, *Asymptotic Expansions* (Academic, New York, 1973), p. 118.